New Insights into the Chemical and Electronic Properties of $C_{69}M$ [M = In^-, Tl^-, Sb^+, Bi^+] Species

Tomekia Simeon,*,† Krishnan Balasubramanian,‡,§,∥ and Jerzy Leszczynski†

Computational Center for Molecular Structure and Interactions, Department of Chemistry, Jackson State University, 1400 JR Lynch Street, P.O. Box 17910, Jackson, MS 39217, Department of Mathematics and Computer Science, California State University, East Bay, Hayward, CA, University of California, Chemistry and Material Science Directorate, Lawrence Livermore National Laboratory, P.O. Box 808 L-268, Livermore, CA 94550, and Glenn T Seaborg Center, Lawrence Berkeley Laboratory, University of California, Berkeley, CA 94720

Received: May 28, 2008; Revised Manuscript Received: September 2, 2008

The replacements of five unique carbons by metal ions within [5,6] fullerene C_{70} D_{5h} has been investigated by using B3LYP/6-31G(d) within 20 isomers of $C_{69}M$ [M = In^-, Tl^-, Sb^+, Bi^+] systems. The equilibrium geometrical structures, relative energies, frontier orbitals, and energy gaps for the four considered series are presented. The obtained results indicate a decrease in effective nuclear charge by addition of an electron, and relativistic effects in $C_{69}Tl^-$ systems causes substantially elongated Tl−C bonds. Variations in the redox characteristics within the four series and among all isomers are expected and also confirmed by Mulliken charges redistributed to neighboring carbon atoms. The vibrational spectra of $C_{69}In^-$ and $C_{69}Sb^+$ have been calculated, which could serve as a framework to interpret future experimental results. Our findings show that substitutional doping of C_{70} with indium, thallium, antimony, and bismuth ions results in interesting properties which can be utilized in the design, synthesis, and growth of nanomaterials in the future.

Introduction

The C_{70} fullerene has received considerable attention as the second largest in abundance and notably the most abundant among higher molecular weight fullerenes present in mass spectra.[1] On the basis of the isolated pentagon rule, C_{70} is predicted to be the second most stable after the celebrated buckminsterfullerene (C_{60}), and it is now well characterized as [5, 6] fullerene C_{70} D_{5h}.[2] Another way to envisage the genesis of C_{70} is that it results from a belt of five hexagons encapsulating the equatorial plane of the C_{60} molecule. Consequently, the overall symmetry of the daughter C_{70} fullerene is reduced to D_{5h}, retaining only one of the five-fold axes; the two hemispheres of C_{60} are rotated by 36° so that they fit contiguously into the belt of hexagons.[3]

There are two remarkable physical characteristics that C_{70} possesses within its framework that makes it distinctly different from C_{60}. The first feature is a consequence of the reduced symmetry, and thus, C_{70} has five unique carbons, whereas in C_{60}, all carbons are equivalent because of the I_h symmetry of the molecule. Also, C_{70} has eight inequivalent bond lengths, whereas in C_{60}, only two distinct types of bonds are found. On the basis of these two distinctions within C_{70}, it is challenging to determine a substitution site for a foreign atom within a modified system like a $C_{69}M$ cluster.

Heterofullerenes are interesting because they serve as precursors to potential new materials for nanotechnology and semiconductors.[4−10] To date, both experimental and theoretical studies have aimed to discover and synthesize these novel nanomaterials.[11−18] The synthesis of these nanomaterials of great potential depends largely on the availability of well-characterized precursor molecular systems, which can assemble into such nanomaterials with considerable promise. Moreover, doping a fullerene such as D_{5h} C_{70} with a Group III anion and a Group V cation could result in interesting properties which can then be utilized in the design, synthesis, and growth of nanomaterials of the future. Furthermore, such metal and metalloid elements are important in many disciplines, such as surface science, metallofullerene, catalysis, inorganic chemistry, and materials science, and thus, many studies have been devoted to a variety of aspects of this subject.[19−23] In the present work, we are particularly interested in clusters composed of semiconductor elements. For example, doping C_{70} with a Group III anion could make an electron-rich system, whereas doping by a Group V cation could make the carbon cage electron-deficient. Consequently, such proposed clusters could act as p-type and n-type semiconductors, respectively. However, exact mechanisms of charge transfers and how the charge is delocalized or distributed over the cage or whether the charge is localized to the substituent neighborhood is far from being understood.

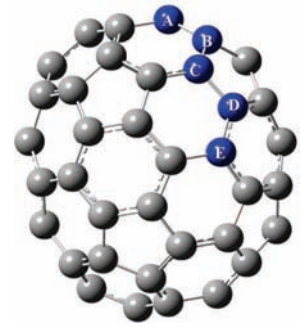

Figure 1. Structure of C_{70}.

* Corresponding author. E-mail: tomekias@ccmsi.us.
† Jackson State University.
‡ California State University.
§ Lawrence Livermore National Laboratory.
∥ University of California.

10.1021/jp804718s CCC: $40.75
Published on Web 10/31/2008

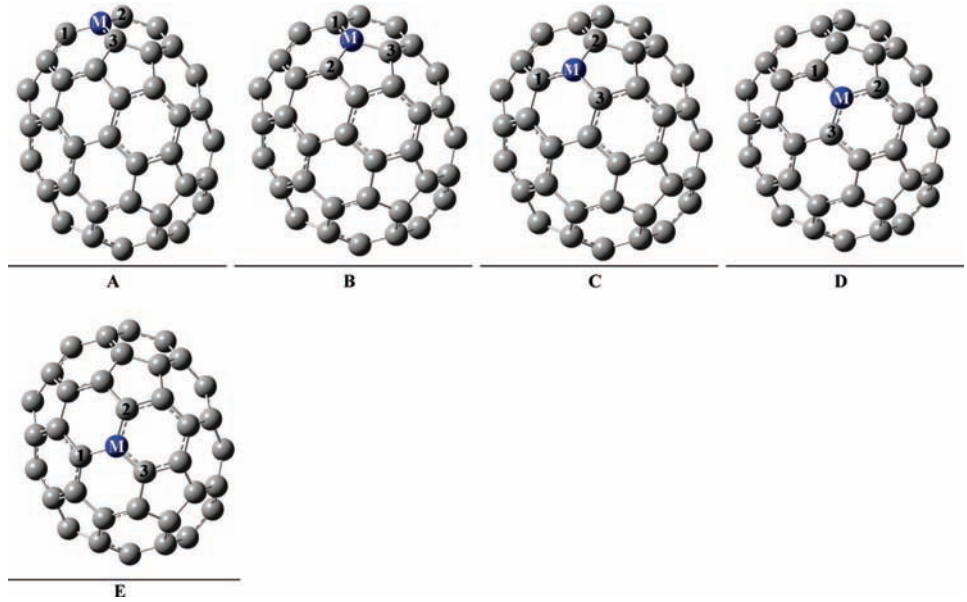

Figure 2. Atomic numeration for neighboring carbons, C1, C2, and C3 bonded to M for isomers A−E.

TABLE 1: Optimized Molecular Parameters for $C_{69}M$ (M = In^-, Tl^-, Sb^+, Bi^+) Isomers Obtained at B3LYP/6-31G*

parameters: bond lengths[a]	$C_{69}In^-$	$C_{69}Tl^-$	$C_{69}Sb^+$	$C_{69}Bi^+$
	Species A			
M−C1	2.07	2.47	2.14	2.30
M−C2	2.01	2.45	2.11	2.27
M−C3	2.07	2.47	2.14	2.30
	Species B			
M−C1	2.04	2.46	2.12	2.28
M−C2	2.11	2.48	2.14	2.29
M−C3	2.11	2.48	2.14	2.29
	Species C			
M−C1	2.01	2.78	2.10	2.26
M−C2	2.09	2.51	2.14	2.29
M−C3	2.08	3.09	2.14	2.29
	Species D			
M−C1	2.05	3.24	2.12	2.27
M−C2	2.07	2.45	2.16	2.31
M−C3	2.04	3.00	2.12	2.27
	Species E			
M−C1	2.08	2.39	2.15	2.31
M−C2	2.01	2.31	2.10	2.26
M−C3	2.01	2.31	2.10	2.26

[a] The bond lengths are in Angstroms.

TABLE 2: Mulliken Atomic Charge Transfer between In^-, Tl^-, Sb^+, and Bi^+ to Carbon Framework Calculated at the B3LYP/6-31G* Level[a]

cluster	q (In) in $C_{69}In^-$	q (Tl) in $C_{69}Tl^-$	q (Sb) in $C_{69}Sb^+$	q (Bi) in $C_{69}Bi^+$
A	0.5805	0.2603	0.8263	0.9598
B	0.5114	0.2404	0.6327	0.9592
C	0.5405	0.2825	0.6255	0.9547
D	0.5917	0.2842	0.6166	0.9569
E	0.5854	0.3804	0.8531	0.9822

[a] Mulliken charges are in atomic units (au).

Furthermore, because of the challenges in experimental synthesis of these types of novel materials, theoretical studies can play a vital role in providing guidance and significant new insights into the structural and electronic properties of these systems. Moreover, relativistic effects could play an important role in bonding and charge transfer properties of some of the heavier cages that we have considered here, and this aspect has not been studied at all up to now. These are some of the motivations of the present study of $C_{69}M$ [M = In^-, Tl^-, Sb^+, Bi^+] systems which have not been studied up to now from the standpoint of structural and electronic properties.

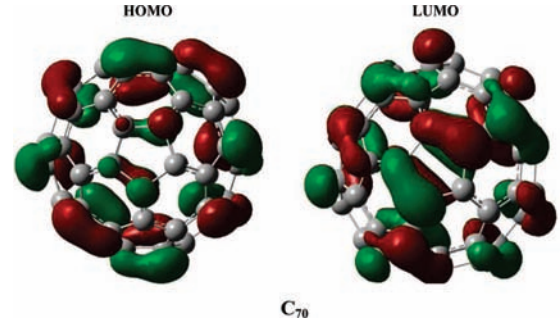

Figure 3. Isocontour plots of HOMO and LUMO for C_{70} obtained at the B3LYP/6-31G* level.

Computational Methods

When considering the size of the structure involved, geometries of all systems were initially optimized without any symmetry constraints by using the hybrid B3LYP functional.[24]

The Kohn−Sham orbitals have been expanded on a Gaussian-type atomic basis set for carbon which is 6-31G(d).[25] For indium, thallium, antimony, and bismuth ions, we have treated the core as a pseudo potential, and only the external electrons are included in the valence band. In particular, for the substituted heteroions, we have used the relativistic effective core potential.[26,27] For indium and antimony, the core space is comprised of 36 electrons, and the valence includes the $4d^{10}5s^25p^2$ and $4d^{10}5s^25p^2$ electrons; we used the basis set reported by LaJohn et. al.[27] For thallium and bismuth atoms, a 68-electron core has been used, and the remaining $5d^{10}6s^26p^2$ and $5d^{10}6s^26p^2$ shells were retained in the valence space together with the basis set reported in reference .

The optimized geometrical parameters, relative energies, frontier orbitals, molecular electrostatic potentials, and energy

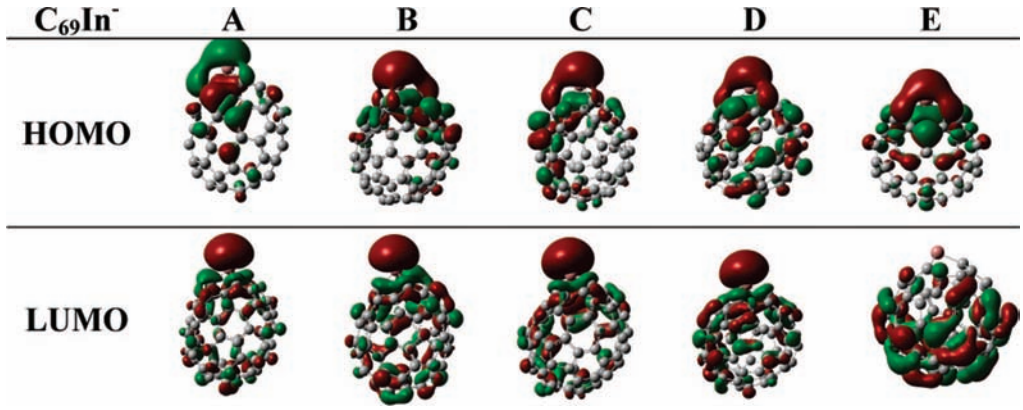

Figure 4. Isocontour plots of HOMO and LUMO for $C_{59}In^-$ clusters obtained at the B3LYP/6-31G* level.

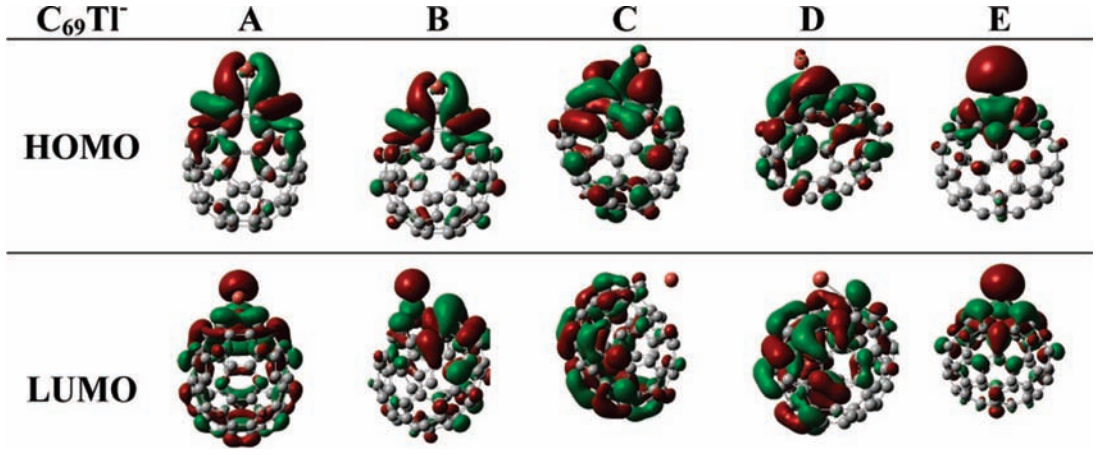

Figure 5. Isocontour plots of HOMO and LUMO for $C_{59}Tl^-$ clusters obtained at the B3LYP/6-31G* level.

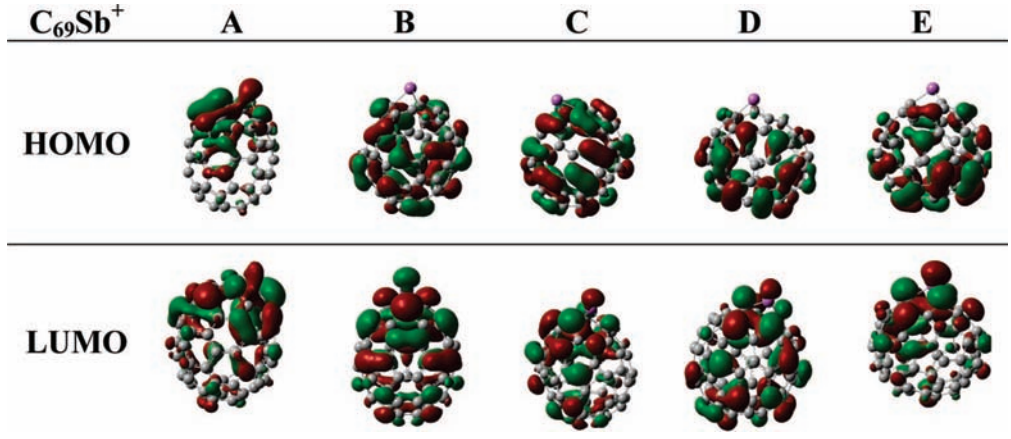

Figure 6. Isocontour plots of HOMO and LUMO for $C_{69}Sb^+$ clusters obtained at the B3LYP/6-31G* level.

gaps for the different systems have been computed. The calculations have been performed by using the Gaussian 03 program package.[29]

Results and Discussion

Computational studies of the various isomers arising from $C_{69}M$ compounds are difficult because of the increased number of carbon atoms and lower symmetry. The lowest energy isomer for C_{70} has D_{5h} symmetry with five unique atomic sites. Doping of indium and thallium anions and antimony and bismuth cations at each unique position resulted in some striking structural patterns and interesting chemical properties. Figure 1 depicts our alphanumeric scheme for labeling of the atomic sites as identified by isomers A−E. Figure 2 shows the position of the substituted ion M [M = In^-, Tl^-, Sb^+, Bi^+], in relation to the neighboring three carbon-atom positions labeled C1, C2, and C3 in Table 1.

All isomers studied had only C_1 symmetry. Because the structure was optimized for each isomer within the DFT method and vibrational frequencies have been obtained for the optimized structures, the reported structures are minima within the DFT formalism and the exchange−correlation hybrid potentials used here.

Table 1 summarizes the calculated bond lengths of $C_{69}M$ [M = In^-, Tl^-, Sb^+, Bi^+] restricted to the neighborhood of the substituted heteroion. An overall trend that we observed is that the metal substitution causes an enlargement of the cage and thus an increase in the surface area and distortion of the carbon

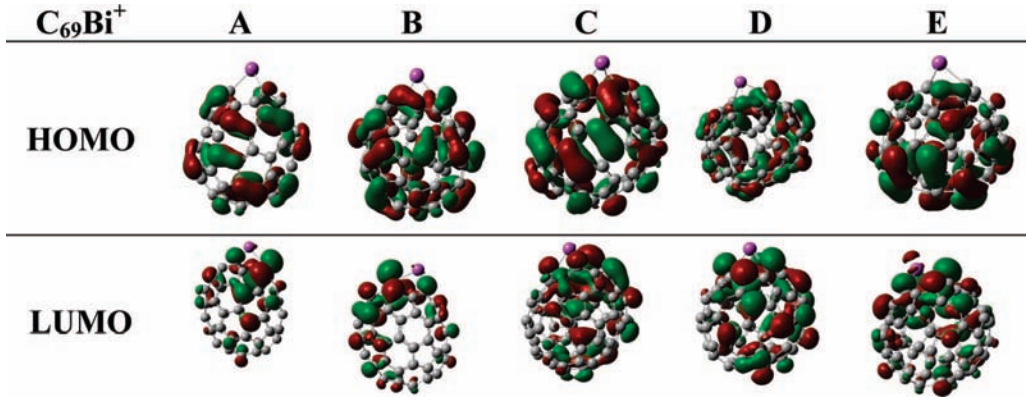

Figure 7. Isocontour plots of HOMO and LUMO for $C_{69}Bi^+$ clusters obtained at the B3LYP/6-31G* level.

TABLE 3: Calculated HOMO, LUMO, and HOMO−LUMO Energy Gaps (ΔE_{H-L}, in eV) Energies, Total Energies (in au), and Dipole Moments (in Debye) at the B3LYP/6-31G*

isomer	HOMO	LUMO	$\Delta E^a{}_{H-L}$	E_{tot}	dipole moment
			$C_{69}In^-$		
A	−2.09	−0.50	1.60	−2631.03817	0.198
B	−2.01	−0.47	1.54	−2631.03037	2.128
C	−2.08	−0.45	1.62	−2631.01973	0.925
D	−1.99	−0.48	1.51	−2631.02417	0.735
E	−2.11	−0.29	1.82	−2631.03159	0.538
			$C_{69}Tl^-$		
A	−2.23	−0.95	1.29	−2680.75182	3.125
B	−2.09	−0.77	1.32	−2680.74943	3.023
C	−1.89	−0.18	1.71	−2680.82112	3.839
D	−1.73	−0.30	1.43	−2680.80056	3.772
E	−2.25	−0.66	1.60	−2680.73718	1.662
			$C_{69}Sb^+$		
A	−8.73	−7.34	1.38	−2634.31018	3.324
B	−8.74	−7.11	1.63	−2634.31359	2.911
C	−8.69	−7.18	1.50	−2634.30387	2.539
D	−8.75	−7.13	1.62	−2634.31168	2.031
E	−8.72	−7.27	1.45	−2634.29859	2.727
			$C_{69}Bi^+$		
A	−8.60	−7.24	1.36	−2701.0817338	4.525
B	−8.59	−6.99	1.60	−2701.0847873	4.065
C	−8.53	−7.07	1.46	−2701.0739063	3.608
D	−8.63	−7.01	1.61	−2701.0820727	3.052
E	−8.60	−7.17	1.43	−2701.0680559	3.817

framework. The equilibrium geometry of C_{70} bond lengths (R_e) range from 1.388−1.473 Å, whereas, as can be seen from Table 1, the M−C distances are 2.01−3.09 Å.

For the calculated bond distances, we have taken the average of the three bond lengths bonded to M [M = In^-, Tl^-, Sb^+, Bi^+] for isomers A−E. The average distances for $C_{69}M$ isomer A are 2.053 Å (In^-), 2.461 Å (Tl^-), 2.133 Å (Sb^+), and 2.287 Å (Bi^+). Comparison of the average R_e of isomers A and B systems suggests that substitution via the latter is not substantially different. For example, changes in distances are 0.016 Å (In^-), 0.014 Å (Tl^-), 0.000 Å (Sb^+), and 0.001 Å (Bi^+). In the case of isolated C_{70}, the various C═C bonds for positions 1−3 change at most by 0.07 Å,[30] indicating that R_e for isomer B systems yield reasonable geometries.

We now compare the geometry of the isomer C with those of the isomers A and B. In comparing the M−C average bond distances, the $^-$Tl−C distance is the longest, as expected. Thallium's elongated bond distances are due to its larger atomic radius. On the other hand, the $^-$In−C, $^+$Sb−C, and $^+$Bi−C

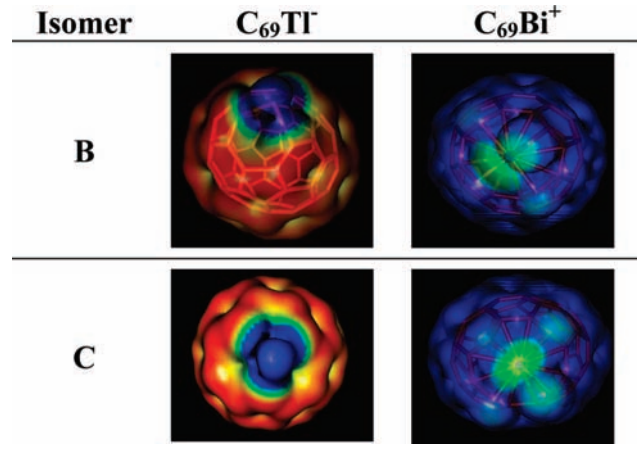

Figure 8. Electrostatic potential plots of $C_{69}M$ [M = Tl^-, Bi^+] for Isomer B and C systems obtained from B3LYP/6-31G* calculations. Blue areas represent positive regions, and red areas represent the most negative regions.

distances are quite similar, $\Delta R_e \leq 0.03$Å. Therefore, this contrast in the behavior of Tl compared to other elements may seem enigmatic on the surface. Thus, we investigated the trend more carefully in light of how relativistic effects may contrast $^-$Tl−C versus $^+$Bi−C bond distances compared to the lighter analogues. In $C_{69}Bi^+$, isomers $^+$Bi−C bond distances are increased by merely 0.12 Å compared to $C_{69}Sb^+$, whereas the difference between Tl−C distance and In−C distance is about 0.4 Å. Although several explanations have been suggested,[31,32] the relativistic effects[33] could play an important role. However, it is puzzling then why $^-$Tl−C should show an elongation of 0.4 Å, whereas $^+$Bi−C bond distance is elongated only by 0.12 Å. This contrast can be rationalized by juxtaposing both relativity and the electronic charges of the heavier atoms. It is well known[33] that the relativistic mass−velocity effect contracts the 6s and $6p_{1/2}$ orbitals of the sixth row elements. In the case of Bi neutral atom, the starting configuration is $6s^26p^3$ from which an electron is removed, which results in $6s^26p^2$ electronic configuration upon ionization of Bi to yield Bi^+. The relativistic contraction of the $6p_{1/2}$ shell which accommodates the two 6p electrons then becomes pronounced once Bi is ionized, resulting in greater effective nuclear charge causing enhanced relativistic shortening, and thus, the $^+$Bi−C and $^+$Sb−C distances are not too far apart. On the other hand, Tl, which is in $6s^26p_{1/2}{}^1$ electronic configuration, added electron increases the electron repulsion in a relativistically contracted $6p_{1/2}$ shell. The relativistic mass−velocity contraction of the $6p_{1/2}$ orbital then renders this semi-inert pair effect, thus causing substantially elongated $^-$Tl−C bonds because of the increase in electron

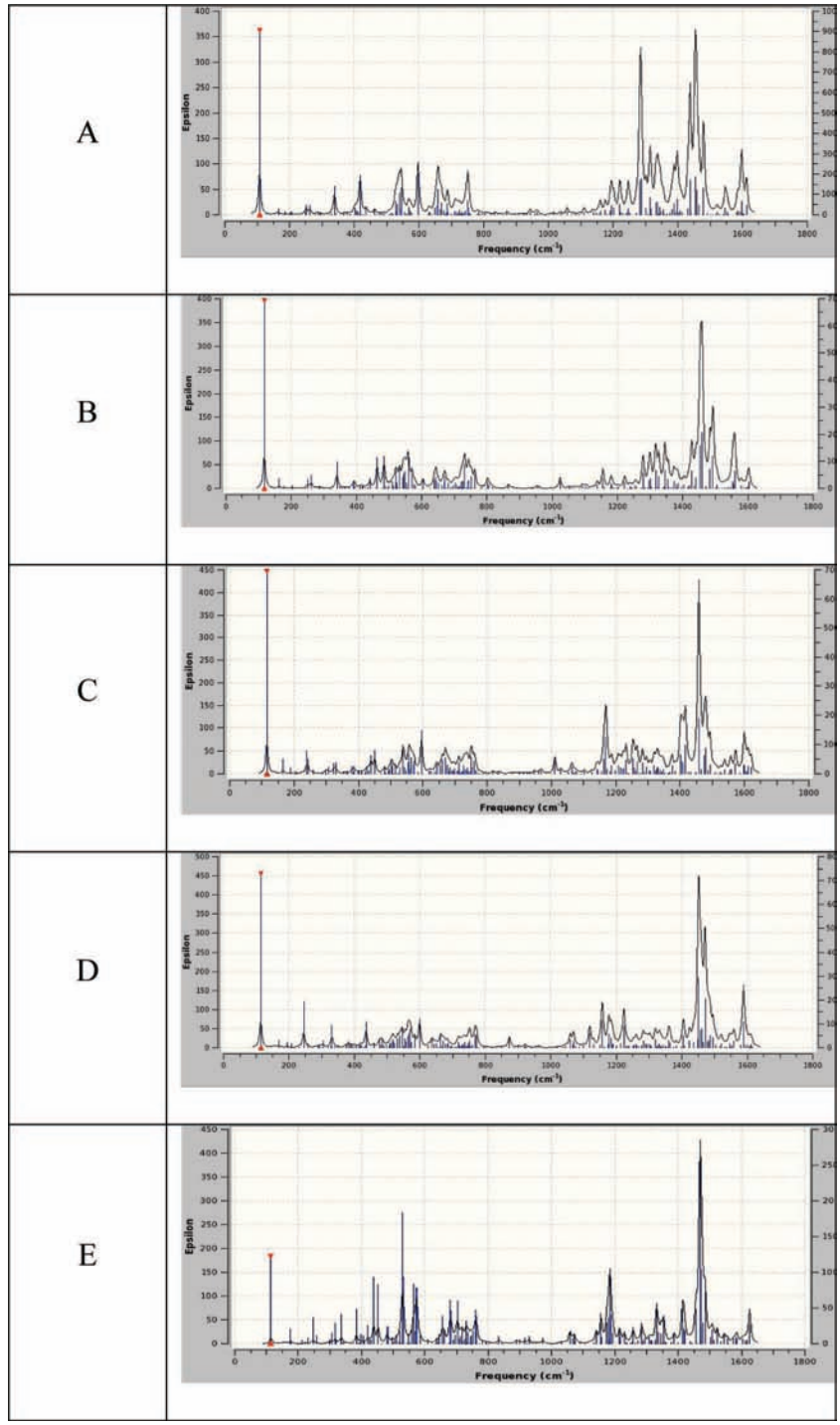

Figure 9. Vibrational spectra for the five isomer structures of $C_{69}In^-$.

repulsion and decrease in effective nuclear charge by added electron. Therefore, substantially longer $^-$Tl−C distances originate from the non-bonding nature of $6p_{1/2}^2$ inert pair configuration of thallium and increased electron repulsion due to an added electron.

Group III and V ions have been forced with $5s^26p^2$ and $6s^26p^2$ atomic valence configurations (verses ns^2np^1 and ns^2np^3) because of charge transfers. In order to shed further light into the effects of charge injection, that is, $C_{69}M^-$[M = In^-, Tl^-] and $C_{69}M^+$, respectively, the calculated Mulliken atomic charges on the substituted atoms and carbon framework are presented in Table 2. They can be used to analyze the electronic charge distribution within A−E isomers.

As can be seen in Table 2 for $C_{69}In^-$ and $C_{69}Tl^-$ isomers, the Mulliken population charges reveal that the added electronic charge on the metal atom is redistributed over the neighboring three carbon (C) atoms. This is in concert with our previous rationalization that the added electron on Tl would cause greater repulsion in the $6p_{1/2}^2$ shell, and thus, the added electronic density is delocalized over the neighbors. Seemingly, the delocalization of charges populated on the three C atoms further suggests that these atoms could serve as potential active sites or react with foreign atoms or other ligands.

In contrast, for Group V isomers, the polarity of M−C bonds is significantly smaller, which also corroborates with the fact that the positive charge on the Group V atom is

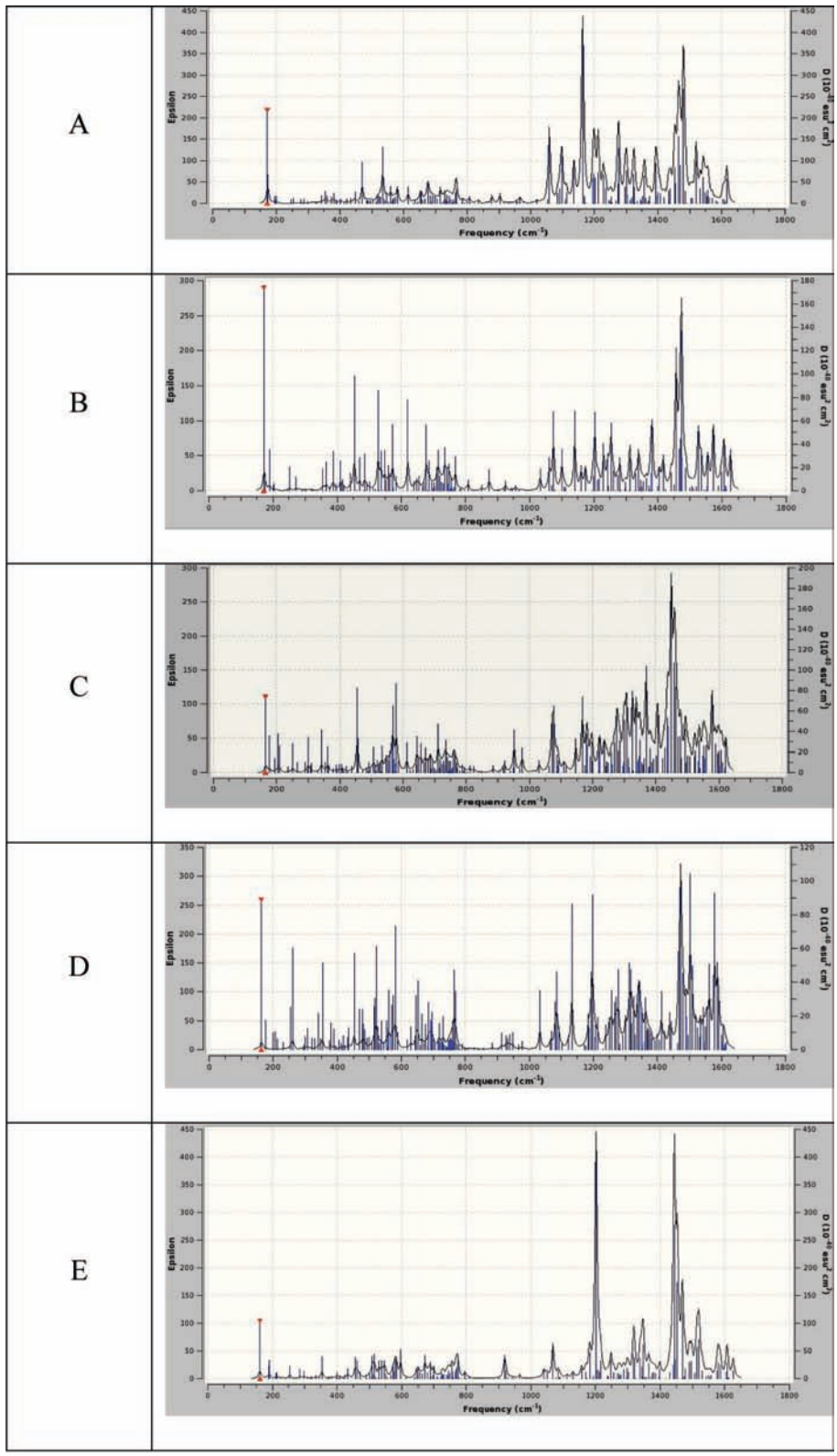

Figure 10. Vibrational spectra for the five isomer structures of $C_{69}Sb^+$.

localized. The Mulliken atomic charges of Sb^+ and Bi^+ within $C_{69}M^+$ are between 0.616 and 0.982 au, whereas for Group III, the charges are 0.282 and 0.596 au. The reduced positive charge for Tl is rationalized on the basis of the inertness of $6p_{1/2}$ orbital, which makes it harder for the electronic charge to be transferred from this orbital of Tl. This also demonstrates that for clusters composed of Group V cationic heteroatoms, the electron transfer to the neighboring three carbons is much less compared to the Group III anionic heteroatoms. The other trend is that charge transfer among Group III anions decreases as one goes down the group. In retrospect, with the exception of $C_{69}Bi^+$ isomers, Mulliken population analysis shows that substantial electronic charge transfers take place through electron donation from the heteroatom to the neighboring carbons. Consequently, increase in the charge densities of carbons would mean that,

if the substituted cage is placed in a solvent, the solubility of the substituted $C_{69}M$ [M= In^-, Tl^-, Sb^+, Bi^+] would be enhanced relative to free C_{70}.

Because frontier orbitals of modified-fullerene-type systems play a vital role in charge transport, we have obtained the electron density distributions of the highest occupied molecular orbital's (HOMOs) and lowest unoccupied molecular orbital's (LUMOs) for C_{70} and all $C_{69}M$ [M = In^-, Tl^-, Sb^+, Bi^+] isomers.

As seen in Figures 3−7, the HOMO and LUMO are mainly dominated by linear combination of atomic orbital's (LCAO) originating from the fullerenes in all cases. Also, the contribution of In^-, Tl^-, Sb^+, and Bi^+ ions into the $C_{69}M$ orbital framework is significant, especially at the substitution site. In Figures 3−7, the green and red colors stand for the positive and negative phases of the MO wave functions, respectively.

For Group III systems, we have observed that the electron density of HOMO and LUMO is localized on the substituted atom for all systems except for the E−$C_{69}In^-$, C−$C_{69}Tl^-$, and D−$C_{69}Tl^-$ isomers. A quite different trend is observed for Group V, because the HOMO and LUMO mainly reside around the carbon framework.

Moreover, the HOMO−LUMO energy separation has been used as a conventional measure of the kinetic stability for various π-electron systems. In general, large HOMO−LUMO gaps are associated with higher kinetic stability, because it is not energetically favorable to add electrons to high-lying LUMO and to extract electron from a low-lying HOMO.

Our calculations reveal that all substituted systems have smaller HOMO−LUMO gaps than C_{70}, which indicates that the addition of In^-, Tl^-, Sb^+, or Bi^+ ions makes the fullerene cage reactive. It can be seen from Table 3 that there is a general trend: the HOMO−LUMO energy gaps decrease from A to B and increase from D to E. In Table 3, it appears that C−$C_{69}Tl^-$ and B−$C_{69}Sb^+$ are the most stable and also have the largest gap within each group of isomers. Also, B−$C_{69}Bi^+$ and D−$C_{69}Bi^+$ are the first and second most stable isomers of that group and have HOMO−LUMO gaps essentially the same. Moreover, the most thermodynamically unstable isomers, C−$C_{69}In^-$, E−$C_{69}Tl^-$, E−$C_{69}Sb^+$, and E−$C_{69}Bi^+$ do not have the smallest ΔE_{H-L}.

For each Group, some remarkable trends are noted; for example, D−$C_{69}In^-$ has the lowest ΔE_{H-L} and differs from the most stable isomer E−$C_{69}In^-$ by 0.20 eV. For Tl^--substituted systems, an energy of 0.42 eV is needed to achieve maximum stability from A−$C_{69}Tl^-$ to C−$C_{69}Tl^-$. When considering the averages for Group III B(13) elements, $C_{69}In^-$ (1.61 eV) and $C_{69}Tl^-$ (1.47 eV), an energy of 0.15eV is needed to promote chemical stability from Tl to In.

Whereas, among $C_{69}Sb^+$ isomers, the difference between the B and A is 0.25eV, for $C_{69}Bi^+$ isomers, the difference between D and A is 0.25 eV. The averages of each series are 1.52 eV for $C_{69}Sb^+$ and 1.49 eV for $C_{69}Bi^+$ isomers. Thus, the stabilization factor from Sb^+ to Bi^+ is only 0.03 eV, whereas, for Group IIIB systems, it increases six-fold. This phenomenon is due to the relativistic effects contributing to the large discrepancy to $C_{69}Tl^-$ systems, which we have already explained on the basis of $6p_{1/2}$ relativistic stabilization.

Figure 8 displays the three dimensional electrostatic potential maps of selected isomers $C_{69}Tl^-$ and $C_{69}Bi^+$, each representative of Group III and V. As can be seen from Figure 8, a highly protruding shape of the potential field at the site of the substitution occurs for both groups. For the $C_{69}Bi^+$ isomer, Bi^+ is engulfed in the framework, and the potential field is shared among neighboring carbons. Furthermore, in $C_{69}Tl^-$, the potential is dispersed among the entire framework.

Replacement of a carbon atom with a metal ion from Group III and V created characteristic changes in the infrared (IR) and Raman spectra. Because of the demand on computing time, the vibration analysis is performed only on $C_{69}In^-$ and $C_{69}Sb^+$ isomers. The results show that all $C_{69}M$ [M = In^-, Sb^+] complexes are local minima because of the absence of imaginary frequencies. Figures 9 and 10 show the calculated IR spectra of the complexes $C_{69}In^-$ and $C_{69}Sb^+$ isomers.

The computational B3LYP spectrum of $C_{69}In^-$ isomers reveals several intense vibrational bands. The strongest absorptions corresponds to the C═C stretching modes of the benzene rings observed in the 1400−1500 cm^{-1} region. For the isomer D, a vibrational mode labeled 177, which corresponds to the C═C bond stretch, exhibits a frequency between 1580−1600 cm^{-1}; this mode has the highest Raman intensity of 107.1289 kcal/mol. There is a significant decrease in this mode's Raman intensity for the other isomers, that is, 4.3815(A), 12.299(B), 2.2717(C), and 0.2077(E) kcal/mol.

The isomer E has the lowest Raman intensities overall for the majority of its vibrations which could be the reason why it has the highest ΔE_{H-L} of 1.8179 eV and thus is the most stable isomer. This would explain isomer E's redshifted peak positions, mode assignments, and intense Raman spectra.

Detailed inspection of the fingerprint region spectra gives weak vibrations at 107.2749 cm^{-1}/24.3789 kcal/mol for A−$C_{69}In^-$, 117.4634 cm^{-1}/20.3873 kcal/mol for B−$C_{69}In^-$, 115.4448 cm^{-1}/ 20.1399 kcal/mol for C−$C_{69}In^-$, and 113.566 cm^{-1}/20.7316 kcal/mol for D−$C_{69}In^-$ isomers. Yet, the identification of the vibrational mode 1 is not as clear, because there is no line of comparable high intensity in the spectra of E−$C_{69}In^-$, that is 113.8174 cm^{-1}.

The fingerprint region features between 400 and 800 cm^{-1} for $C_{69}In^-$ systems are more pronounced for the isomers A and E, whereas for B, C, and D, broad bands are extended up to 800 cm^{-1}.

It can be seen from Figure 10 that the exact line position as well as the number of resolved individual lines in $C_{69}Sb^+$ isomers differ more strongly than in the case of $C_{69}In^-$ cages. Isomers A and E have two sharp peaks at 1163.1791 and 1480.5910 and 1201.5811 and 1443.8826 cm^{-1} for E. The values of these peaks correspond to the intensity of a carbon double-bond stretching, which explains why these two isomers display lower stabilities, which is evident from their ΔE_{H-L} of 1.3556 and 1.430 eV, respectively. Thus, as the kinetic stability decreases for a system, the intensity of mode assignments decreases and further red-shifts the spectra.

Conclusions

Molecular structure and properties of the $C_{69}M$ [M = In^-, Tl^-, Sb^+, Bi^+] have been investigated. Twenty different types of local minima structures of the doped systems were found. It was shown that the bonds between $C_{69}M$ are elongated and much weaker than the bonds of the cluster. The main feature, in retrospect to the isomers, is that the bond lengths increase monotonically down the groups, and considerable change induced by the heteroatom bond angles could facilitate breaking the framework. Mulliken population analysis reveals that a stronger interaction between closely packed $C_{69}M$ molecules would be more stable than C_{70}. The HOMO−LUMO energy gaps of all $C_{69}M$ clusters which are associated with the chemical stability against electronic excitation are generally smaller than those of C_{70}, suggesting that an electron in $C_{69}M$ is more easily

excited from HOMO−LUMO than in C_{70}. The vibrational spectra for $C_{69}In^-$ and $C_{69}Sb^+$ have also been calculated. In order to assist in such experimental studies, theoretical IR spectra have been calculated to determine molecular vibrations which are specific to the particular local minima of antimony and indium in $C_{69}M$.

Acknowledgment. This research was supported in part by the U.S. Department of Energy under Grant No. DE-FG02-04ER15546 and ONR Grant no. N000140810324. The work at Lawrence Livermore National Laboratory was performed under the auspices of U.S. Department of Energy under Contract No. AC52-07NA27344.

References and Notes

(1) Dresselhaus, M. S.; Dresselhaus, G.; Eklund, P. C. *Science of Fullerenes and Carbon Nanotubes*; Academic Press: New York, 1996.
(2) Diederich, F.; Ettl, R.; Rubin, Y.; Whetten, R.; Beck, R.; Alvarez, M.; Anz, S.; Sensharma, D.; Wudl, F.; Khemani, K.; Koch, A. *Science* **1991**, *252*, 548.
(3) Turker, L. *J. Mol. Struct.* **2002**, *619*, 107.
(4) Guo, T.; Jin, C.; Smalley, R. E. *J. Phys. Chem.* **1991**, *95*, 4948.
(5) Pradeep, T.; Vijayakrishnan, V.; Santra, A. K.; Rao, C. N. R. *J. Phys. Chem.* **1991**, *95*, 10564.
(6) Lamparth, I.; Nuber, B.; Schick, G.; Skiebe, A.; Groesser, T.; Hirsch, A. *Angew. Chem., Int. Ed. Engl.* **1995**, *34*, 2257.
(7) Ying, Z. C.; Hettich, R. L.; Compton, R. N.; Haufler, R. E. *J. Phys. B* **1996**, *29*, 4935.
(8) Andreoni, W.; Gygi, F.; Parrinello, M. *Chem. Phys. Lett.* **1992**, *190*, 159.
(9) Xia, X.; Jelski, D. A.; Bowser, J. R.; George, T. F. *J. Am. Chem. Soc.* **1992**, *114*, 6493.
(10) Hummelen, J. C.; Knight, B.; Pavlovich, J.; Gonzalez, R.; Wudl, F. *Science* **1995**, *269*, 1554.
(11) Kurita, N.; Koboyyashi, K.; Kumabora, H.; Tago, K.; Ozawa, K. *Chem. Phys. Lett.* **1992**, *198*, 95.
(12) Bowser, J. R.; Jeleski, D. A.; George, T. F. *Inorg. Chem.* **1992**, *31*, 154.
(13) Wang, S. H.; Chen, F.; Fann, Y. C.; Kashani, M.; Malaty, M.; Jansen, S. A. *J. Phys. Chem.* **1995**, *99*, 6801.
(14) Zhoug, S. J.; Liu, C. W. *J. Mol. Struct. (Theochem)* **1997**, *392*, 125.
(15) Chen, Z.; Ma, K.; Chen, L.; Zhao, H.; Pan, Y.; Zhao, X.; Tang, A.; Feng, J. *J. Mol. Struct. (Theochem)* **1998**, *452*, 219.
(16) Chen, Z.; Ma, K.; Pan, Y.; Zhao, X.; Tang, A.; Feng, J. *J. Chem. Soc. Farad. Trans.* **1998**, *94*, 2269.
(17) Chen, Z.; Zhao, X. *J. Phys. Chem. A.* **1999**, *103*, 10961.
(18) Yang, X.; Wang, G. C.; Shang, Z. F.; Pan, Y. M.; Cai, Z. S.; Zhao, X. Z. *Phys. Chem. Chem. Phys.* **2002**, *4*, 2546.
(19) Martin, T. P. *Phys. Rep.* **1983**, *95*, 167.
(20) Phillips, J. C. *Chem. Rev.* **1986**, *86*, 619.
(21) Halperin, W. P. *Rev. Modern Phys.* **1986**, *58*, 533.
(22) Salahub, D. R. *Adv. Chem. Phys.* **1987**, *69*, 447.
(23) Kappes, M. M. *Chem. Rev.* **1988**, *88*, 369.
(24) Becke, A. D. *Phys. Rev. A* **1988**, *38*, 3098.
(25) Raghavachari, K.; Trucks, G. W. *J. Chem. Phys.* **1989**, *91*, 1062.
(26) Pacious, L. F.; Christiansen, P. A. *J. Chem. Phys.* **1985**, *82*, 2664.
(27) LaJohn, L. A.; Christiansen, P. A.; Ross, R. B.; Atashroo, T.; Ermleu, W. C. *J. Chem. Phys.* **1987**, *87*, 2812.
(28) Wildman, S. A.; Dilabio, G. A.; Christiansen, P. A. *J. Chem. Phys.* **1997**, *107*, 9975.
(29) Frisch, M. J.; Trucks, G. W.; Schlegel, H. B.; Gill, P. M. W.; Johnson, B. G.; Robb, M. A.; Cheeseman, J. R.; Keith, T.; Petersson, G. A.; Montgomery, J. A.; Raghavachari, K.; Al-Laham, M. A.; Zakrzewski, V. G.; Ortiz, J. V.; Foresman, J. B.; Cioslowski, J.; Stefanov, B. B.; Nanayakkara, A.; Challacombe, M.; Peng, C. Y.; Ayala, P. Y.; Chen, W.; Wong, M. W.; Andres, J. L.; Replogle, E. S.; Gomperts, R.; Martin, R. L.; Fox, D. J.; Binkley, J. S.; Defrees, D. J.; Baker, J.; Stewart, J. P.; Head-Gordon, M.; Gonzalez, C.; Pople, J. A. *Gaussian 94*, revision E.2; Gaussian, Inc.: Pittsburgh, PA, 1995.
(30) Diederich, F.; Ettl, Y.; Rubin, *Science* **1991**, *252*, 548.
(31) Hargittai, M. *Chem. Rev.* **2000**, *100*, 2233.
(32) Virko, S.; Petrenko, T.; Yaremko, A.; Wysokinski, R.; Michalska, D. *J. Mol. Struct. (Theochem)* **2002**, *582*, 137.
(33) Balasubramanian, K. *Relativistic Effects in Chemistry*; Wiley Interscience, 1997; Parts A and B.

JP804718S